JACS
JOURNAL OF THE AMERICAN CHEMICAL SOCIETY
Communication
pubs.acs.org/JACS

Thermally Triggered Self-Assembly of Folded Proteins into Vesicles

Won Min Park and Julie A. Champion*

School of Chemical & Biomolecular Engineering, Georgia Institute of Technology, Atlanta, Georgia 30332, United States

Supporting Information

ABSTRACT: We report thermally triggered self-assembly of folded proteins into vesicles that incorporates globular proteins as building blocks. Leucine zipper coiled coils were combined with either globular proteins or elastin-like polypeptides as recombinant fusion proteins, which form "rod−coil" and "globule-rod−coil" protein complex amphiphiles. In aqueous solution, they self-assembled into hollow vesicles via temperature-responsive inverse phase transition. The characteristic of the protein vesicle membranes enables preferential encapsulation of simultaneously formed protein coacervate. Furthermore, the type of encapsulated cargo extends to small molecules and nanoparticles. Our approach offers a versatile strategy to create protein vesicles as vehicles with biological functionality.

Vesicles are enclosed compartments created by self-assembled membranes of amphiphiles. While biological vesicles made from amphiphilic small molecules, predominantly phospholipids, are abundant in nature, their macromolecular analogues have been developed primarily using synthetic block copolymers.[1] Polymeric vesicles exhibit enhanced stability and mechanical properties,[2] and their permeability,[3] size,[4] and shape[5] can be tuned. Besides synthetic block copolymers, biological copolymers, such as polypeptides[6,7] and recombinant proteins,[8] have also been developed to self-assemble into vesicles. They are biocompatible and biodegradable and can offer biofunctionality through incorporation of peptide sequences or folded proteins. Self-assembly of folded proteins, in many examples, provides a versatile method to fabricate functional biomaterials for a range of applications.[9,10] However, direct incorporation of folded and biologically relevant moieties into protein amphiphiles can prevent conformational arrangement of chains during vesicle formation, and their molecular weight might be limited. Furthermore, organic solvents, which are typically added to dissolve amphiphilic proteins or polypeptides,[6,8] can hamper biological activity of incorporated folded proteins. For these reasons, vesicles of folded recombinant proteins are underdeveloped.[8] In fact, folded, globular proteins have been incorporated into vesicles only as hybrid forms of protein-synthetic polymers.[11] Herein, we report self-assembly of vesicles from recombinant protein amphiphiles that contain folded globular proteins. In aqueous solution, formation of hollow vesicles with globular proteins results from temperature-responsive phase transition. Depending on the conditions, vesicles can encapsulate protein coacervates formed simultaneously. In addition, small molecules and nanoparticles can preferentially be encapsulated in the vesicles.

An elastin-like polypeptide (ELP) motif serves as the hydrophobic block. It is a penta-repeat polypeptide derived from tropoelastin that undergoes an inverse phase transition, from soluble to insoluble, in aqueous solution as temperature increases above the transition temperature.[12] It is an attractive process to construct various nanostructures via thermally triggered self-assembly. When combined with hydrophilic domains, amphiphilic diblocks containing ELP motifs have led to formation of spherical[13,14] and cylindrical micelles[15] and vesicles.[16] While random coil peptides were used as hydrophilic blocks in most examples, rigid, rod-shaped leucine zipper coiled coils and globular proteins are used here. Combined with an ELP, the folded proteins are incorporated into self-assembled vesicles as part of the building blocks.

In the present study, protein vesicles were created by combinations of three different diblock recombinant proteins: Z_R−ELP, mCherry−Z_E, and EGFP−Z_E (Figure 1A). An ELP motif was conjugated with a coiled coil domain (Z_R) as a fusion protein Z_R−ELP.[17] The arginine-rich leucine zipper motif (Z_R) forms coiled coil complexes with its counterpart Z_E.[18] The glutamic acid-rich leucine zipper motif (Z_E) was fused with two different fluorescent proteins, mCherry[19] and EGFP. As illustrated in Figure 1, panel B, the leucine zipper coiled coil

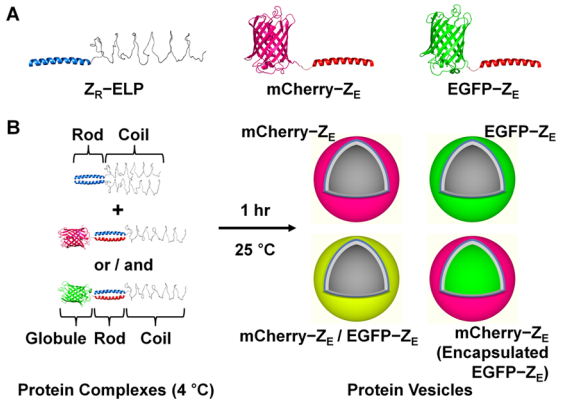

Figure 1. Recombinant protein amphiphiles and their self-assembly into vesicles. (A) Recombinant diblock copolypeptides: Z_R−ELP, mCherry−Z_E, and EGFP−Z_E (PDB ID: 2H5Q for mCherry and 1EMK for EGFP). (B) The rod−coil (Z_R−ELP homodimer) and globule-rod−coil (mCherry−Z_E/Z_R−ELP and EGFP−Z_E/Z_R−ELP) protein complexes prepared in solution at 4 °C self-assemble into hollow vesicles employing mCherry, EGFP, or both globular domains. Depending on conditions, EGFP−Z_E can form a coacervate phase encapsulated by mCherry−Z_E vesicles.

Received: September 1, 2014
Published: December 11, 2014

dx.doi.org/10.1021/ja5090157 | J. Am. Chem. Soc. 2014, 136, 17906−17909

(Z_E/Z_R) incorporates the globular domains into a "globule-rod–coil" protein complex (mCherry–Z_E/Z_R–ELP or EGFP–Z_E/Z_R–ELP) via its high affinity interaction with extremely low dissociation constant ($K_d \approx 10^{-15}$ M).[18] Because of the weaker affinity between Z_R motifs ($K_d \approx 10^{-7}$ M),[18] Z_R–ELP forms homodimers and was used as a temperature-responsive "rod–coil" protein amphiphile. The globule-rod–coil and rod–coil protein complex amphiphiles are made first by mixing (Figure 1B), where the globular and rod-shaped proteins serve as hydrophilic blocks. Circular dichroism spectroscopy confirms that each protein complex contains the α-helical coiled coil motifs (Figure S2).

By incubating the protein mixture at room temperature, ELP separates into a hydrophobic phase, and the protein complexes self-assemble into vesicles in aqueous solution (Figure 1B). The protein mixture solution, prepared at 4 °C, was placed at room temperature for an hour and became turbid as a result of vesicle formation (Figure S3). Figure 2, panels A and B show protein

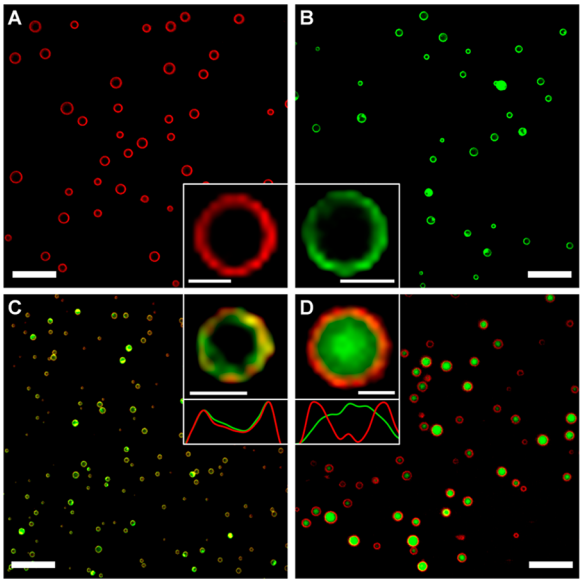

Figure 2. Self-assembled protein vesicles. Confocal micrographs of vesicles prepared from solutions containing different concentrations of the recombinant protein components: (A) 1.5 μM of mCherry–Z_E and 30 μM of Z_R–ELP; (B) 0.6 μM of EGFP–Z_E and 30 μM of Z_R–ELP; (C) 0.3 μM of mCherry–Z_E, 0.3 μM of EGFP–Z_E, and 30 μM of Z_R–ELP; (D) 1.5 μM of mCherry–Z_E, 0.6 μM of EGFP–Z_E, and 30 μM of Z_R–ELP. Salt concentrations of the solutions were (A) 0.30 M, (B,C) 0.91 M, and (D) 0.45 M. Fluorescence from the vesicles was visualized using different colors, red (mCherry–Z_E) and green (EGFP–Z_E), which colocalize to yellow in panel C. The insets are close-up images, and the curves in panels C and D are fluorescence intensity profiles corresponding to the inset images. Scales bars are 10 and 1 μm (inset), respectively.

vesicles self-assembled from Z_R–ELP mixed with either mCherry–Z_E or EGFP–Z_E. According to dynamic light scattering (DLS) measurements (Figure 5A), the average diameters were 1.26 and 1.82 μm for vesicles incorporating mCherry and EGFP domains, respectively, with a narrow size distribution (polydispersity index <0.03). The red and green fluorescence indicates homogeneous incorporation of mCherry–Z_E and EGFP–Z_E in each vesicle membrane. Since the inverse phase transition of ELP does not involve use of any organic solvents and thus provides a biocompatible environment, no loss of fluorescence by denaturation of mCherry or EGFP was seen. Upon dilution of the vesicle solution, no significant change in fluorescence intensity was observed (Figure S5), which indicates that mCherry–Z_E is not exchanged between vesicles and solution due to the extremely low dissociation constant of Z_E and Z_R coiled coils. To confirm that the vesicles are hollow, we imaged cross-sections of fractured, freeze-dried vesicles. Scanning electron microscopy (SEM) images clearly show the empty inner space of a vesicle (Figure S6). Thickness of the vesicle membrane, measured from SEM images, was about 20 nm.

We found salt concentration to be a critical factor for vesicle formation. We tested the inverse phase transition of protein mixture solutions at different salt concentrations (0.15 M–1.21 M) with a fixed concentration of Z_R–ELP (30 μM). Vesicle formation was only observed above critical values of salt concentration, which are estimated to be approximately 0.30 and 0.91 M for vesicles incorporating mCherry–Z_E and EGFP–Z_E, respectively. Below these concentrations, we only observed formation of coacervate particles, droplets of protein-rich phases (Figure S4). They are the typical result of ELP inverse phase transition.[20,21]

As probed by turbidity profiles, molecular packing of vesicles is distinct from that of coacervate particles (Figure 3A). After an

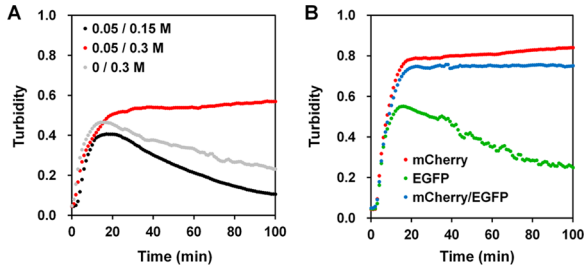

Figure 3. Turbidity profiles of protein solutions during inverse phase transition. The optical density at 400 nm was monitored at 25 °C from the solutions prepared at 4 °C. (A) Molar ratio of mCherry–Z_E to Z_R–ELP (χ) was 0.05 and 0 at different salt concentrations (0.15 and 0.30 M). (B) Protein solutions contain 1.5 μM of mCherry–Z_E (red), 0.6 μM of EGFP–Z_E (green), and both (blue) at salt concentration of 0.45 M. All protein solutions contain 30 μM of Z_R–ELP.

initial rapid increase, saturation of turbidity was observed at the salt concentrations for vesicle formation. It indicates that the surface of vesicles is hydrophilic and stable, which can be achieved via packing of the rod and globule-rod protein blocks. However, there was a slow decrease in turbidity when formation of coacervate particles was favored, either at lower salt concentrations or in the absence mCherry–Z_E or EGFP–Z_E. This decrease is caused by coalescence of protein coacervate particles,[20] which indicates that they have hydrophobic surfaces where ELP motifs are exposed to water.

The effect of salt concentration can be further rationalized using the packing parameter, $P = V/(a_0 l_c)$.[22] V is the volume of the hydrophobic (ELP) block, a_0 is the average head area of the hydrophilic block, and l_c is the critical length (Figure 4A). The hydrophilic part is composed of the globular domain (mCherry or EGFP) and the rod-shaped coiled coils (mixtures of Z_R/Z_R homodimers or Z_E/Z_R heterodimers). When mCherry–Z_E (or EGFP–Z_E) is mixed with Z_R–ELP, the average head area per single strand of ELP (a_0) is expressed as $a_0 = (1 - \chi)a_1/2 + \chi a_2$, where χ is the molar ratio of mCherry–Z_E (or EGFP–Z_E) to Z_R–ELP, and a_1 and a_2 are the head areas of Z_R/Z_R and

dx.doi.org/10.1021/ja5090157 | J. Am. Chem. Soc. 2014, 136, 17906–17909

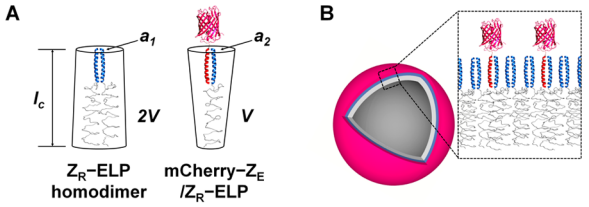

Figure 4. Molecular packing of protein complex amphiphiles. (A) Truncated cone models for Z_R–ELP homodimer and mCherry–Z_E/Z_R–ELP to explain the packing parameter *P*. (B) A proposed model of single-layer vesicular membrane.

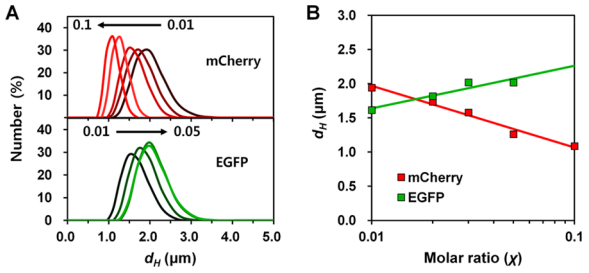

Figure 5. Hydrodynamic diameter (d_H) of vesicles with different molar ratios (χ). (A) Size distribution obtained from DLS measurement. Molar ratio of mCherry–Z_E to Z_R–ELP (top), 0.01, 0.02, 0.03, 0.05, 0.1; EGFP–Z_E to Z_R–ELP (bottom), 0.01, 0.02, 0.03, 0.05. Concentration of Z_R–ELP was fixed at 30 μM for all samples at different salt concentrations: 0.30 M (mCherry–Z_E vesicles) and 0.91 M (EGFP–Z_E vesicles). (B) The corresponding correlation between χ and d_H of vesicles containing mCherry–Z_E (red) and EGFP–Z_E (green).

mCherry(EGFP)–Z_E/Z_R, respectively (Figure 4A). Because of fixed secondary structure and surface properties of the globule and rod blocks, a_0 should not strongly depend on salt concentration. In contrast, *V* is significantly influenced by ionic strength. According to conformational mechanics of ELPs,[23] ELP molecules are more collapsed with increasing salt concentration. Therefore, increased ionic strength reduces *V* and decreases the packing parameter *P*. In this sense, the protein amphiphiles have an inverted cone shape that forms coacervate particles when $P > 1$, below the critical values of salt concentration. Above the critical values, *V* is reduced, and vesicle formation is favored at $1/2 < P < 1$. Therefore, conformational dependency of ELP on ionic strength seems strongly related to morphologies of the aggregates made from the protein amphiphiles.

Moreover, our argument based on the packing parameter clearly explains why the critical salt concentration is dependent on the type of globular domains. As demonstrated, *P* is also dependent on the average head area a_0 that changes as a function of the molar ratio χ and a_2. Importantly, the head area a_2 is decided by the nature of globular domains, as they are covalently linked to Z_E/Z_R coiled coils (Figure 4A). For example, mCherry is a monomeric and highly soluble globular protein,[24] and a_2 becomes larger than the head area resulted only from a coiled coil ($\sim a_1$) because of steric hindrance provided by the conjugated mCherry domain. In contrast, EGFP tends to dimerize at millimolar concentration[25] or even can aggregate as indicated by the bright spots observed in Figure 2, panel B. The attraction between EGFP domains reduces a_2 corresponding to EGFP–Z_E/Z_R block. Thus, the salt concentration required for $1/2 < P < 1$ should be higher for EGFP than mCherry.

Our observations on the correlation between χ and the average hydrodiameter of vesicles (d_H) strongly evidence the influence of globular domains on the packing parameter *P*. With increasing χ at a given salt concentration, d_H of mCherry–Z_E vesicles decreased, while we observed an increase in d_H of EGFP–Z_E vesicles (Figure 5). The increased curvature of mCherry–Z_E vesicles at higher χ indicates $a_2 > a_1$ and $a_2 < a_1$ for EGFP–Z_E vesicles, since their curvature decreases with increasing χ. Thus, mCherry provides a larger head area (a_2) than EGFP, since a_1 is independent of the globular domains. These opposite trends, with equally increased fractions of Z_E/Z_R coiled coils in both systems, indicate that influence from the globular domains seems to be dominant over interactions between Z_R/Z_R and Z_E/Z_R coiled coil domains. Nonetheless, various interactions between the protein domains may exist and contribute to self-assembly.

When vesicle formation conditions are favorable for both globular domains, we found that both mCherry–Z_E and EGFP–Z_E were incorporated into membrane of hollow vesicles (Figure 2C). Surprisingly, at a condition where only formation of mCherry–Z_E vesicles is favored, the two globular domains separated into different microphases within a vesicle (Figure 2D). The confocal micrograph indicates that mCherry–Z_E and Z_R–ELP self-assembled into vesicles whose interior is filled with EGFP–Z_E and Z_R–ELP. Different from the hollow vesicles incorporating both globular domains in the membrane, this condition resulted in vesicles with "core–shell" morphology. According to the observed morphological dependence on salt concentration, the vesicular layer composed of mCherry–Z_E and Z_R–ELP encapsulates the coacervate phase of EGFP–Z_E and Z_R–ELP, which was simultaneously formed during the inverse phase transition. Again, as probed by turbidity profiles, the saturation in turbidity after phase transition indicates that the "shell" is a stable vesicular membrane of tightly packed protein amphiphiles (Figure 3B). At the same salt concentration, however, the turbidity profile for the mixture of only EGFP–Z_E and Z_R–ELP showed a gradual decrease, which indicates formation of typical coacervate particles. This demonstrates that vesicles incorporating multiple types of globular domains in either the membrane or interior compartment can self-assemble by adjusting salt concentration.

Preferential encapsulation of the coacervate phase could be explained by a hypothetical model of vesicles composed of a self-assembled "single-layer" membrane. It is distinguished from "bilayer" membranes of typical block copolymer vesicles. In a bilayer, hydrophilic chains are both inside and outside of vesicles. In our proposed model, the hydrophobic ELP blocks face the interior (Figure 4B), and the inner surface could stabilize the encapsulated protein coacervate phase. An example of synthetic rod–coil block copolymers demonstrates that they form hollow aggregates where a hydrophobic inner shell encapsulates hydrophobic cargo.[26] Despite the globular domains included in our system, this example shares the same characteristic of rod-shaped blocks directly interfaced with hydrophobic coil blocks. We hypothesize that the rigid, rod-shaped conformations could maintain a low interfacial curvature between the coiled coils and ELP[6] and may prevent collapse of hollow structure even in the absence of encapsulated coacervate phase. Moreover, our observation of correlation between packing parameter and curvature of vesicles (Figure 5) is similar to a characteristic of single-layer superstructures assembled from mesoscopic metal–polymer amphiphiles.[27]

In addition to protein coacervate, encapsulation of small molecules can be simply achieved by mixing with the protein amphiphiles, followed by inverse phase transition. As a model

dx.doi.org/10.1021/ja5090157 | J. Am. Chem. Soc. 2014, 136, 17906–17909

molecule, fluorescein was mixed with mCherry−Z_E and Z_R−ELP at 4 °C and warmed to room temperature. As a result, the inner space of resulting vesicles was filled with fluorescein, as shown in the confocal micrograph (Figure 6A). The level of fluorescein was maintained, which indicates low permeability through the vesicle membrane.

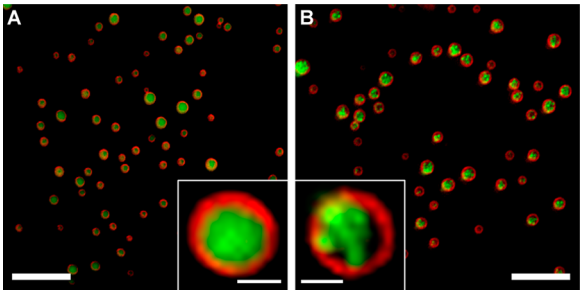

Figure 6. Encapsulation of cargo by protein vesicles. Confocal micrographs of vesicles encapsulating (A) fluorescein and (B) polystyrene nanoparticles. Vesicles of mCherry−Z_E (1.5 μM) and Z_R−ELP (30 μM) were self-assembled in the presence of fluorescein (50 μg/mL) or fluorescent polystyrene nanoparticles with diameters of 500 nm (125 μg/mL). Salt concentration was 0.45 M. The green color indicates fluorescence from (A) fluorescein and (B) polystyrene nanoparticles, while fluorescence from mCherry−Z_E is visualized by red. The insets are close-up images. Scales bars are 10 and 1 μm (inset), respectively.

Importantly, when mCherry−Z_E vesicles were assembled in the presence of carboxylated fluorescent polystyrene nanoparticles (diameter ∼500 nm), we observed the nanoparticles located inside the resulting vesicles (Figure 6B). The confocal micrograph shows the green fluorescent particles surrounded by the red fluorescent vesicular membrane. This result could be explained if the vesicle membrane provides a hydrophobic inner wall. Considering the low number density and length scale of the nanoparticles relative to vesicles, encapsulation should be driven by attractive interactions between the hydrophobic nanoparticles and inner wall of the membrane. Indeed, the protein vesicles can encapsulate cargo with multiple length scales: small molecules ($\sim 10^0$ nm), proteins ($\sim 10^1$ nm), and nanoparticles ($\sim 10^2$ nm).

In conclusion, we describe the aqueous self-assembly of protein vesicles that incorporate globular domains as building blocks via temperature-responsive inverse phase transition. It provides a versatile method to fabricate protein vesicles in biocompatible environments. Thus, folded and biologically functional proteins, such as enzymes or receptor ligands, could be incorporated into vesicle membranes for practical applications. Importantly, the simple and efficient encapsulation of various types of cargo will provide an opportunity for many applications in drug delivery.

■ ASSOCIATED CONTENT

Supporting Information

Experimental details, protein sequences, and characterization data about protein purification, secondary structure, vesicle formation and morphology, and protein coacervate. This material is available free of charge via the Internet at http://pubs.acs.org.

■ AUTHOR INFORMATION

Corresponding Author

julie.champion@chbe.gatech.edu

Notes

The authors declare no competing financial interest.

■ ACKNOWLEDGMENTS

This research was financially supported by the National Science Foundation (1032413) and Georgia Tech Emory Center for Regenerative Medicine. We acknowledge Profs. D. Tirrell and K. Zhang for DNA plasmids and Prof. N. Hud for technical assistance with circular dichroism spectroscopy.

■ REFERENCES

(1) Discher, D. E.; Eisenberg, A. *Science* **2002**, *297*, 967.
(2) Discher, B. M.; Won, Y.-Y.; Ege, D. S.; Lee, J. C.-M.; Bates, F. S.; Discher, D. E.; Hammer, D. A. *Science* **1999**, *284*, 1143.
(3) Battaglia, G.; Ryan, A. J.; Tomas, S. *Langmuir* **2006**, *22*, 4910.
(4) Luo, L.; Eisenberg, A. *Langmuir* **2001**, *17*, 6804.
(5) Meeuwissen, S. A.; Kim, K. T.; Chen, Y.; Pochan, D. J.; van Hest, J. C. M. *Angew. Chem., Int. Ed.* **2011**, *50*, 7070.
(6) Bellomo, E. G.; Wyrsta, M. D.; Pakstis, L.; Pochan, D. J.; Deming, T. J. *Nat. Mater.* **2004**, *3*, 244.
(7) Holowka, E. P.; Pochan, D. J.; Deming, T. J. *J. Am. Chem. Soc.* **2005**, *127*, 12423.
(8) Vargo, K. B.; Parthasarathy, R.; Hammer, D. A. *Proc. Natl. Acad. Sci. U.S.A.* **2012**, *109*, 11657.
(9) Hudalla, G. A.; Sun, T.; Gasiorowski, J. Z.; Han, H.; Tian, Y. F.; Chong, A. S.; Collier, J. H. *Nat. Mater.* **2014**, *13*, 829.
(10) Leng, Y.; Wei, H.-P.; Zhang, Z.-P.; Zhou, Y.-F.; Deng, J.-Y.; Cui, Z.-Q.; Men, D.; You, X.-Y.; Yu, Z.-N.; Luo, M.; Zhang, X.-E. *Angew. Chem., Int. Ed.* **2010**, *49*, 7243.
(11) Amado, E.; Schöps, R.; Brandt, W.; Kressler, J. *ACS Macro Lett.* **2012**, *1*, 1016.
(12) Urry, D. W.; Trapane, T. L.; Prasad, K. U. *Biopolymers* **1985**, *24*, 2345.
(13) Dreher, M. R.; Simnick, A. J.; Fischer, K.; Smith, R. J.; Patel, A.; Schmidt, M.; Chilkoti, A. *J. Am. Chem. Soc.* **2007**, *130*, 687.
(14) Kim, W.; Thévenot, J.; Ibarboure, E.; Lecommandoux, S.; Chaikof, E. L. *Angew. Chem., Int. Ed.* **2010**, *49*, 4257.
(15) Lee, T. A. T.; Cooper, A.; Apkarian, R. P.; Conticello, V. P. *Adv. Mater.* **2000**, *12*, 1105.
(16) Martín, L.; Castro, E.; Ribeiro, A.; Alonso, M.; Rodríguez-Cabello, J. C. *Biomacromolecules* **2012**, *13*, 293.
(17) Zhang, K.; Sugawara, A.; Tirrell, D. A. *ChemBioChem* **2009**, *10*, 2617.
(18) Moll, J. R.; Ruvinov, S. B.; Pastan, I.; Vinson, C. *Protein Sci.* **2001**, *10*, 649.
(19) Park, W. M.; Champion, J. A. *Angew. Chem., Int. Ed.* **2013**, *52*, 8098.
(20) Cirulis, J. T.; Keeley, F. W. *Biochemistry* **2010**, *49*, 5726.
(21) Osborne, J. L.; Farmer, R.; Woodhouse, K. A. *Acta Biomater.* **2008**, *4*, 49.
(22) Israelachvili, J. N. *Intermolecular and Surface Forces: Revised Third ed.*; Elsevier Science: Waltham, MA, 2011.
(23) Valiaev, A.; Lim, D. W.; Schmidler, S.; Clark, R. L.; Chilkoti, A.; Zauscher, S. *J. Am. Chem. Soc.* **2008**, *130*, 10939.
(24) Lam, C. N.; Kim, M.; Thomas, C. S.; Chang, D.; Sanoja, G. E.; Okwara, C. U.; Olsen, B. D. *Biomacromolecules* **2014**, *15*, 1248.
(25) Zacharias, D. A.; Violin, J. D.; Newton, A. C.; Tsien, R. Y. *Science* **2002**, *296*, 913.
(26) Jenekhe, S. A.; Chen, X. L. *Science* **1998**, *279*, 1903.
(27) Park, S.; Lim, J.-H.; Chung, S.-W.; Mirkin, C. A. *Science* **2004**, *303*, 348.